Numerical method for energy absorption maximization in latice structures and experimental validation

NUMERICAL METHOD FOR ENERGY ABSORPTION MAXIMIZATION IN LATTICE STRUCTURES AND EXPERIMENTAL VALIDATION

Stefania Liseni [(1)], Antonio Coluccia [(1)], Guillaume Meyer [(2)], Christian Mittelstedt [(2)], Giorgio De Pasquale [(1)]

[(1)] Smart Structures and Systems Lab, Dept. of Mechanical and Aerospace Engineering, Politecnico di Torino, Corso Duca degli Abruzzi 24, Torino 10129, Italy
Email: stefanialiseni@outlook.it, antonio.coluccia@polito.it, giorgio.depasquale@polito.it
[(2)] Lightweight Engineering and Structural Mechanics, Dept. of Mechanical Engineering, Technical University of Darmstadt, Otto-Berndt-Straße 2, Darmstadt 64287, Germany
Email: guillaume.meyer@klub.tu-darmstadt.de, christian.mittelstedt@klub.tu-darmstadt.de

KEYWORDS

Lattice structures, energy absorption, structural grading.

ABSTRACT

Lattice structures, and in general cellular solids, show good propensity to energy absorption capability and lightweight. These advanced materials are obtaining attention in research fields such as aerospace and automotive, where their functionalization and mechanical properties provide a valid alternative to traditional viscoelastic materials and energy absorbers. In lattice structures, the macroscale mechanical properties can be tailored through their mesoscale configuration and in particular the topology of the unit cells.
This investigation is aimed at the definition of a pre-sizing tool for the maximization of the energy absorption of lattice structures, and consequently the homogenization of the stress distribution inside the lattice. To this end, a structural grading process has been developed: according to the initial stress state of the lattice, thicknesses of the struts are varied, generating a new graded configuration that shows enhanced mechanical properties. Finally, validating experiments are performed.

1. INTRODUCTION

Mechanical properties of cellular solids and lattice structures have been investigated in the last decades [1] [2]. The interest around these materials and structures is motivated by their excellent performances and functionality in different fields of engineering, such as aerospace and automotive engineering, or biomedical applications. Together with their excellent mechanical properties and versatility, lattices also present many advantages from the point of view of lightweight engineering, presenting a relative density which is variable according to the objective they are supposed to achieve.
Research literature is rich with investigations about the employment of lattices in the aerospace field: in [3], lattices are used as fillers for the design of the anti-icing system of an aircraft wing. Here, both the energy absorption and heat management properties of lattices plays an important role. Such structures are also the object of interest in the field of heat exchange [4]. Cylindrical shells, often used for the construction of spacecraft bodies are often manufactured using lattice structures, both for their lightweight and the possibility they offer to accommodate different instrumentations. The structural integrity of the attachment points of such lattice cylinders is investigated in [5], while fatigue analysis is performed on the same structures in [6]. An investigation of their axial deformability can be found in [7]. Lattice-like amorphous metal panels subjected to impact load are studied in [8], where these cellular unit panels are meant to be used to protect spacecrafts from micro-meteoroids and orbital debris impacts.
Both the mechanical properties and the functionality of lattices are employed for different designs meant to achieve different objectives [9]. The design freedom in building lattice structures is also due to additive manufacturing, which allows extremely complex topologies to be manufactured using different metal alloys. One of the most investigated properties in lattices is energy absorption [10] [11]; typically, the finite element method (FEM) is among the most employed tools for its study, often supported by the experimental validation of calculation results. Optimization of such properties, together with other mechanical ones, is also a topic of interest in research literature, and it can be performed through different means. In [12], lattices of different topology are employed together in the same sample according to specific rules in order to maximize energy absorption, generating a multi-morphology design. Also, the topology and shape of the single cell can

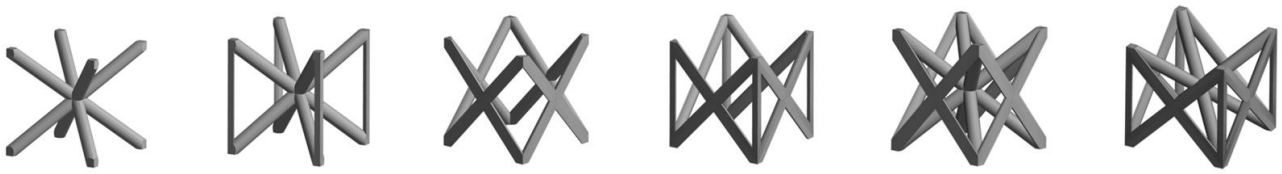

Figure 1: Cell topologies selected, from left to right, bcc, bccz, fcc, fccz, fbcc, fbccz

be modified in order to optimize specific property, as in [13]. Structural grading is also a useful tool for the optimization of mechanical properties, for different load conditions: in [14] a graded design is presented for tensile specimens, while [15] presents how bidirectional grading can work properly for compressive loads.
This investigation employs structural grading, therefore the modification of the thicknesses of the lattices involved, based on the stress state acting in the lattices in an ungraded configuration, aimed at the enhancement of energy absorption properties. External mathematical fields that are not based on the actual stress state of the lattices are not used in this study, as well as no black-box-optimizers are involved in this investigation. Finally, the experimental validation of the process is provided.

2. MODEL AND NUMERICAL ANALYSIS

Lattice topologies selected for the investigation are *bcc, bccz, fcc, fccz, fbcc and fbccz*. Such topologies allow the study of both different orientation angles of the struts, combination of different cells and vertical reinforcement. Cells are shown in Fig. 1. The bilinear material model used for the simulation is based on AlSi10Mg alloy. Both cells and material model used are taken from a previous investigation [10] for consistency; the reference parameters of the model can be found there. Each single representative volume element (RVE) of the lattice presents a constant edge length of 3 mm and it corresponds to one cell; also, for every lattice, strut diameter of ungraded configurations is 0.37 mm. A cubic sample composed of 10x10x10 cells is considered for each topology.

2.1. Compression bilinear simulations

The first step of the process consists in performing a compressive static simulation for each sample. Ansys Workbench software is employed for the simulations. A bilinear material model for AlSi10Mg is used, associated to 2-noded beam elements for the struts modeling. Based on a sensitivity analysis, each strut is defined through two elements. Boundary conditions applied are meant to simulate a fixed and a crushing plate: the nodes at the lower surface of the sample are completely fixed, while -2 mm displacement (compression) is imposed to the nodes at the upper surface. First important outputs of these simulations are force-displacement diagrams, later converted into stress-strain diagrams by dividing the force to the section area and the displacement to the sample edge length. From these diagrams, volumetric energy absorption (*VEA*), energy absorption (*EA*) and specific energy absorption (*SEA*) are calculated by means of Eqs. 1-3. Here, σ is the nominal stress obtained from the force reaction, ε is the strain obtained from the displacement, *V* is the volume of the sample and *m* is its mass.

$$VEA = \int_0^{\varepsilon} \sigma(\varepsilon) d\varepsilon \quad (1)$$

$$EA = VEA * V \quad (2)$$

$$SEA = EA/m \quad (3)$$

Secondly, a local equivalent stress, evaluated according to Eq.4, is defined throughout the whole sample for each strut via user defined output formulation in Ansys.

$$\sigma_e = \left|\sigma_{direct} + \sigma_{bendingMAX}\right| \quad (4)$$

In Eq.4, σ_{direct} is the axial stress along the beam, while $\sigma_{bendingMAX}$ is the maximum bending stress registered (between the two possible bending axes) for the element. For each cell of the lattice, the maximum equivalent stress is registered, generating a 3D map of the maximum equivalent stresses, on which the whole grading process is based.

2.2. The grading process

The grading process is based on the variation of the strut diameters, according to different rules and hypotheses; the whole process is aimed at the homogenization of the stress within the lattice sample, and therefore the maximization of energy absorption. Two different processes are developed, where the only difference between them is the third hypothesis.
The first hypothesis is the strain equivalence principle: both the ungraded and the graded

sample, that is a result of the maximization process, are subjected to the same displacement, therefore strain. Also, stresses on which are based the process are due to this same strain. The second hypothesis is the force reaction dependency to the equivalent stress distribution: the reaction that a single cell is applying depends on the maximum equivalent stress inside that cell, therefore the total force reaction of the sample depends on the distribution of the maximum equivalent stress achieved in each cell. The third hypothesis only valid for process 1, is the geometrical dependency: the force reaction is proportional to the average relative density of the sample (that changes accordingly to the zone of the sample, being this one graded). On the contrary, the third hypothesis only valid for process 2 is the geometrical independency: the force reaction remains constant when the grading process is applied, despite the relative density variation. Based on these hypotheses, two different equations, respectively for process P1 (Eq. 5) and process P2 (Eq. 6) are defined. Process P1 is expected to be more impactful on the mechanical properties than process P2, resulting in heavier lattices. Process P2 could be useful for application where lightweight is the priority; while process P1 could be useful for applications where high mechanical properties and high *EA* is strictly required despite higher relative density.

$$t_{P1} = \sqrt{\left(\frac{\sigma_{e,MAX}}{\sigma_{eT}}\right)\left(\frac{\rho_R}{\rho_{R0}}\right)t_0^2} \quad (5)$$

$$t_{P2} = \sqrt{\left(\frac{\sigma_{e,MAX}}{\sigma_{eT}}\right)t_0^2} \quad (6)$$

Therein, t is the struts diameter, ρ_R is the relative density, and values with subscript *0* are properties of the ungraded configuration. For Eq. 5, ρ_R can be expressed through t according to a specific equation that employs coefficients evaluated via interpolation. This equation and coefficients can be found in [10]. This expression is applied for the single cell of the lattice sample, therefore $\sigma_{e,MAX}$ is the maximum equivalent stress registered for that cell. σ_{eT} is the equivalent stress threshold, used for the normalization of the stress term of the expressions. A threshold is useful for the selection of the cells on which to apply the processes: all of the cells that present a maximum equivalent stress higher than the threshold are object to diameter modifications. Thresholds chosen for this investigation are:

- *T1*: 25% above the level of the average maximum stresses registered in each cell of the sample; only few cells exceed this threshold, therefore improvement of mechanical process is limited as well as the increase of the sample mass.
- *T2*: minimum of the maximum stresses registered in each cell of the sample; except few cells, the whole sample is object to grading, resulting in high performances at the cost of a relevant mass increase.
- *T3*: average of the maximum stresses registered in each cell of the sample; this threshold is a compromise between the previous two.

A Matlab code, used for the application of the grading process, is also used to evaluate the energetic parameters of the graded configurations of the samples, without the need to perform finite element simulations again.

3. EXPERIMENTAL VALIDATION

The most promising samples from the point of view of energy absorption improvement, that are *bcc* and *bccz* (see results in section 4), are validated by an experimental campaign. Samples are produced in both their ungraded and graded configurations P1 and P2 for threshold *T3*.

For each configuration, 5 samples (plus one for the ungraded one) are produced. Those have been manufactured at the Institute of Lightweight Engineering and Structural Mechanics of the Technical University of Darmstadt, employing an EOS M290 selective laser melting machine, by means of AlSi10Mg powder. As-built samples are

Figure 2: compression test of the bccz sample graded using process P1

Table 1:results from bilinear static simulations

	bcc	***bccz***	***fcc***	***fccz***	***fbcc***	***fbccz***
Force reaction [N]	1635.6	7447.4	4795.9	10224	7740.8	13351
EA [mJ]	683.1	3356.1	1917	4266	2937.6	5445.9
VEA [mJ]	0.0253	0.1243	0.0710	0.1580	0.1088	0.2017
SEA [mJ/g]	114.0	477.0	356.2	663.86	258.4	438.7

rather brittle, hence a heat treatment consisting of an annealing at 350°C for 2 hours is performed.
Static compression tests are performed for each sample according to the German standard DIN 50134. The machine employed for the tests is the ZwickRoell Z100. Lattice structures are compressed along their print direction and the samples were investigated at a strain rate of 0.3mm/min. The compression tests are stopped once the samples reach 66% strain. VEA and SEA are defined by Eqs. 1 and 3. Results from experiments can be found in the next section, together with a comparison between them and data from the computational models, while pictures taken during the compression test of the bccz sample graded using P1 cam be seen in Fig. 2.

4. RESULTS AND DISCUSSION

Tab.1 reports the energetic parameters obtained from initial bilinear static simulation for ungraded samples. They are in line with previous investigations [10] made about the same lattice topologies. *Fbccz* is the cell that performs best for *VEA* and *EA*, and this is also due to its high relative density. On the other hand, *fccz*, being lighter than *fbccz*, is the best cell from the point of view of *SEA*. Vertical reinforcement always plays an important role in enhancing the energetic properties of such lattices.
SEA and *VEA* percentage increases for all of the graded samples, using both process P1 and P2 and all of the thresholds, as presented in Tab. 2. It can be immediately noted how the general trend is for lattices with lower relative density to be more sensitive to the increase of energetic properties. Also, in most cases, vertically reinforced lattices show lower increases with respect to their non-reinforced counterparts. *VEA* and *SEA* enhancements are far higher for process P1 rather than P2. This result was expected since process P1 is based on the dependance of the force reaction on the relative density, and *EA* is in order dependent on the force reaction. This is also an issue dependent on the employment of a specific threshold: when using *T1*, thicknesses obtained from modifications are much lower than the ones obtained with the other two thresholds, therefore obtaining much lower *SEA* and *VEA* increases. The main point about *T1* is that very few cells exceed in maximum equivalent stress the value above the 25% of the average of the maximum equivalent stress registered in each cell, therefore very few cells are subject to the grading process. The behavior is completely opposite to *T2*: here basically all of the cells exceed the threshold, therefore all of the samples undergo the grading

Table 2: SEA and VEA increments with respect to ungraded configurations for both processes and all the thresholds

Sample	***T1***		***T2***		***T3***	
	***SEA* increase**	***VEA* increase**	***SEA* increase**	***VEA* increase**	***SEA* increase**	***VEA* increase**
bcc P1	+8.16%	+14.62%	+97.97%	+373.52%	+62.09%	+168.77%
bcc P2	+7.11%	+7.51%	+125.72%	+404.74%	+10.76%	+16.60%
bccz P1	+9.30%	+17.14%	+92.47%	+355.84%	+48.55%	+120.51%
bccz P2	+7.01%	+7.61%	+51.69%	+127.59%	+12.64%	+17.70%
fcc P1	+5.01%	+9.15%	+99.01%	+376.21%	+54.36%	+140.71%
fcc P2	+7.01%	+7.32%	+70.63%	+189.15%	+8.42%	+12.96%
fccz P1	+1.54%	+2.53%	+86.47%	+326.58%	+25.61%	+55.13%
fccz P2	+8.05%	+9.10%	+15.80%	+33.54%	+9.75%	+11.90%
fbcc P1	+0.59%	+1.10%	+75.95%	+321.24%	+18.15%	+41.91%
fbcc P2	+4.46%	+4.50%	+54.20%	+136.42%	+5.31%	+7.54%
fbccz P1	+0.10%	+0.25%	+72.24%	+305.56%	+19.29%	+46.75%
fbccz P2	+0.93%	+0.94%	+35.99%	+84.18%	+4.78%	+7.34%

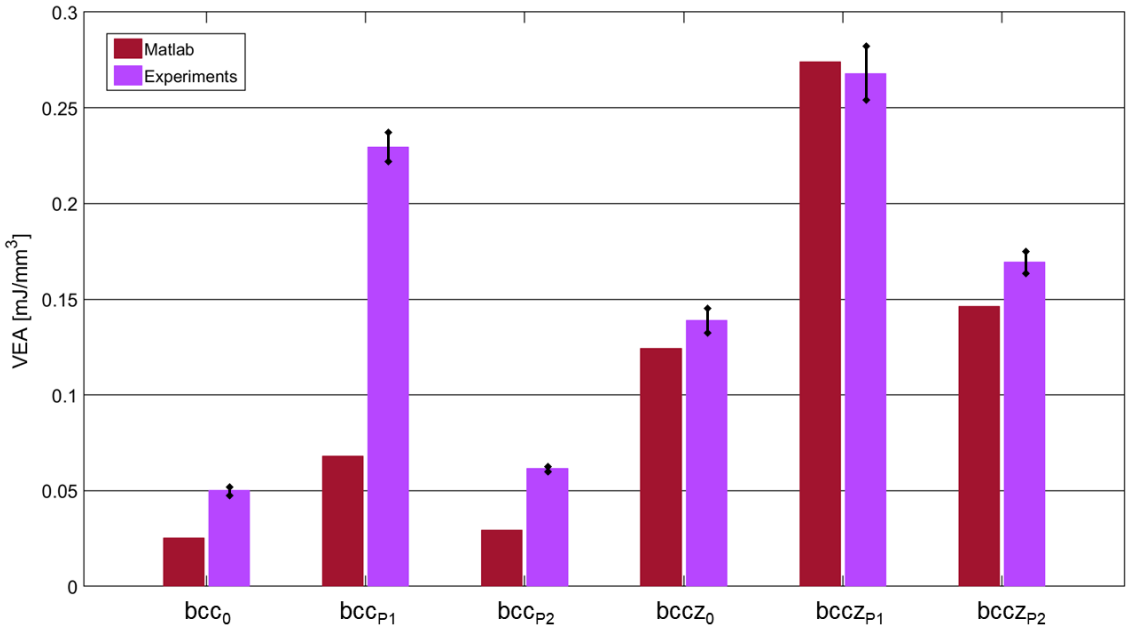

Figure 3: VEA obtained from the Matlab code and from experiments (at the same strain as the model)

process. Though best results in term of SEA and VEA are obtained with this threshold, the strut diameter is sometimes so high that the concept of lattice structure is completely lost, and the sample is composed of bulk material only ($\rho_R \approx 1$). *T3* offers instead good results together with a proper thickness distribution; the concept of lattice structure is in fact still respected. Of course, the three thresholds, chosen for the demonstrative application of the grading process presented in this paper, can be modulated according to the user preferences and according to the desired level of invasiveness of the process to the original lattice structure.

Figs. 3 ad 4 shows comparisons between *VEA* and *SEA* obtained from the graded samples (averaged) evaluated through Matlab and the same energetic values obtained from experimental tests (only for *bcc* and *bccz* configurations). The employment of the Matlab code for the evaluation of the energetic

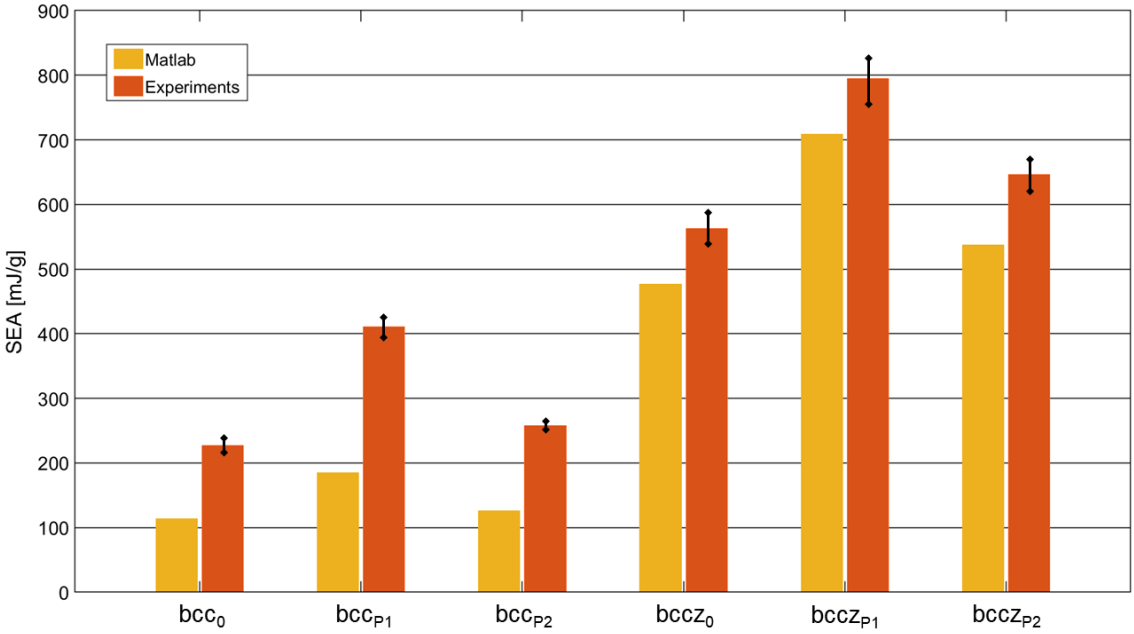

Figure 4: SEA obtained from the Matlab code and from experiments (at the same strain as the model)

properties of processed lattices is an advantage: the code only takes some minutes to complete the calculations, while Ansys takes from the 3 to 8 hours to complete the simulation on a calculator with the same hardware setup (without considering time for the post-processing of results). Trends are the same between the two ways properties are evaluated. The most evident differences are the discrepancies between the values for bcc configurations, both graded and ungraded. This difference could be due to different issues: the employment of beam elements, that are less accurate of solid elements in the representation of the struts. Also, force reaction estimation for compression loading from simulations works better for lattices presenting vertical struts, being aligned with the load direction itself; this could be the reason behind the discrepancy between energy parameters evaluated via software and from experiments. Another issue is the difference between the actual properties of heat treated AlSi10Mg and the properties employed for its bilinear model used for FEM simulations; variances could also be due to the accuracy of the printing process and the deviation of manufactured lattices from nominal dimensions. Also, simulations do not consider contact friction between plates and sample, resulting in a slight difference that is part of the discrepancy between results from experiments and from the model. Being nevertheless the trend and the magnitude of the results obtained the same between results from Matlab and from experiments, it can be said that the validation campaign is successful, and the model works properly.

It can be stated that the grading process obtained is able to produce modifications in the strut thickness distribution that produces an important increase in the energetic properties. This process also presents the possibility to modulate the impact of the strut modification on the original structure, according to the preferences of the user, that could employ the process for different application aims. Presently, the process also presents limitations: the variation of the strut thickness happens for a whole cell and not at the level of the single strut. Through better stress homogenization, therefore, energy absorption enhancement could be obtained once making the process work on the single struts.

5. CONCLUSIONS

A tool for lattice structures grading in the optic of improving their energy absorption properties has been developed obtaining good results: by using a proper threshold for the selection of the cell to be modified, the process achieved up to the +168% *VEA* increase and +62% *SEA* increase (both for *bcc*). Also, according to the user preferences and objectives, the process can be performed at different levels, choosing the right threshold in order to achieve a more or less relevant impact on the lattice properties or relative density. It can also be concluded that the employment of the Matlab code for the evaluation of the energetic properties of the graded lattices is timesaving, with respect to repeating the same analyses with the FEM.

Beside the results achieved in this investigation, the tool can of course be improved, for example by letting the process work on the single struts. Further investigations could be conducted about employing this grading process on an applicative case study.

6. REFERENCIES

1. M. F. Ashby, “Mechanical Properties of Cellular Solids.,” *Metall. Trans. A, Phys. Metall. Mater. Sci.*, vol. 14 A, no. 9, pp. 1755–1769, (1983), doi: 10.1007/BF02645546.

2. V. S. Deshpande, N. A. Fleck, and M. F. Ashby, “Effective properties of the octet-truss lattice material,” *J. Mech. Phys. Solids*, vol. 49, pp. 1747–1769, (2001).

3. G. De Pasquale and A. Tagliaferri, “Modeling and characterization of mechanical and energetic elastoplastic behavior of lattice structures for aircrafts anti-icing systems,” *Proc. Inst. Mech. Eng. Part C J. Mech. Eng. Sci.*, vol. 235, no. 10, pp. 1828–1839, (2021), doi: 10.1177/0954406219853857.

4. X. Wang, Z. Zhong, T. Zeng, G. Xu, Y. Cui, and K. Zhang, “Heat transfer property of C/SiC composite pyramidal lattice core sandwich structures,” *Compos. Struct.*, vol. 301, no. September, p. 116215, (2022), doi: 10.1016/j.compstruct.2022.116215.

5. B. J. R. Smeets *et al.*, “Structural testing of a shear web attachment point on a composite lattice cylinder for aerospace applications,” *Compos. Part B Eng.*, vol. 212, no. November 2020, p. 108691, (2021), doi: 10.1016/j.compositesb.2021.108691.

6. Y. Kim, I. Kim, and J. Park, “An approximate formulation for the progressive failure analysis of a composite lattice cylindrical panel in aerospace applications,” *Aerosp. Sci. Technol.*, vol. 106, p. 106212, (2020), doi: 10.1016/j.ast.2020.106212.

7. A. V. Lopatin, E. V. Morozov, and A. V. Shatov, “Axial deformability of the composite lattice cylindrical shell under compressive loading: Application to a load-carrying spacecraft tubular body,” *Compos. Struct.*, vol. 146, pp. 201–206, (2016), doi: 10.1016/j.compstruct.2016.03.021.

8. M. Davidson *et al.*, “Investigating amorphous metal composite architectures as spacecraft

shielding," *Adv. Eng. Mater.*, vol. 15, no. 1–2, pp. 27–33, (2013), doi: 10.1002/adem.201200313.
9. A. Seharing, A. H. Azman, and S. Abdullah, "A review on integration of lightweight gradient lattice structures in additive manufacturing parts," *Adv. Mech. Eng.*, vol. 12, no. 6, pp. 1–21, (2020), doi: 10.1177/1687814020916951.
10. A. Coluccia, G. Jiang, G. Meyer, G. De Pasquale, and C. Mittelstedt, "Nonlinear static and dynamic modeling of energy absorption lattice structures behavior," *Mech. Adv. Mater. Struct.*, (2022), doi: 10.1080/15376494.2022.2064016.
11. T. Maconachie *et al.*, "The effect of topology on the quasi-static and dynamic behaviour of SLM AlSi10Mg lattice structures," *Int. J. Adv. Manuf. Technol.*, vol. 118, no. 11–12, pp. 4085–4104, (2022), doi: 10.1007/s00170-021-08203-y.
12. R. Alberdi *et al.*, "Multi-morphology lattices lead to improved plastic energy absorption," *Mater. Des.*, vol. 194, p. 108883, (2020), doi: 10.1016/j.matdes.2020.108883.
13. G. Bertolino, M. Montemurro, and G. De Pasquale, "Multi-scale shape optimisation of lattice structures: an evolutionary-based approach," *Int. J. Interact. Des. Manuf.*, vol. 13, no. 4, pp. 1565–1578, (2019), doi: 10.1007/s12008-019-00580-9.
14. G. Meyer, K. Schelleis, O. Weeger, and C. Mittelstedt, "Tensile specimen design proposal for truss-based lattice structures," *Mech. Adv. Mater. Struct.* (2022), doi: 10.1080/15376494.2022.2097352.
15. J. Yang *et al.*, "Compressive properties of bidirectionally graded lattice structures," *Mater. Des.*, vol. 218, p. 110683, (2022), doi: 10.1016/j.matdes.2022.110683.